Lamb Wave Resonators based on Co-sputtered $Al_{0.78}Sc_{0.22}N$ Thin Film

Zhifang Luo[*†‡], Shuai Shao[*†‡], and Tao Wu[*†‡]
Email: luozhf@shanghaitech.edu.cn; wutao@shanghaitech.edu.cn;
[*]School of Information Science and Technology, ShanghaiTech University, Shanghai, China
[†]Shanghai Institute of Microsystem and Information Technology, Chinese Academy of Sciences, Shanghai, China
[‡]University of Chinese Academy of Sciences, Beijing, China
[‡]Shanghai Engineering Research Center of Energy Efficient and Custom AI IC, Shanghai, China

***Abstract*—This paper reports the lamb wave resonator based on co-sputtered $Al_{0.78}Sc_{0.22}N$ thin film. High-quality $Al_{0.78}Sc_{0.22}N$ thin film with a 1.8° FWHM of (0002) polarization is achieved by magnetron co-sputtering. The process of Inductively Coupled Plasma (ICP) etching is discussed. Optimized ICP etching recipe is characterized to achieve relatively vertical etching profile. The device structure is optimized to improve the quality factor utilizing finite element analysis (FEA) based on perfectly matched layer (PML) in COMSOL Multiphysics®. $Al_{0.78}Sc_{0.22}N$ lamb wave resonators operating at around 300 MHz are fabricated. A resonator with electromechanical coupling coefficient (k_t^2) over 5% and loaded quality factor (Q) of 1219 is obtained, which exhibits a figure of Merit (FOM) of 63.88.**

***Keywords*— MEMS, AlScN, lamb wave resonator**

I. Introduction

Piezoelectric Microelectromechanical System (MEMS) has attracted much attention in wireless communications[1]–[3]. In the past few decades, a wide variety of piezoelectric materials have been investigated, such as Aluminum Nitride (AlN)[4], [5], Lithium Niobate (LN)[6], [7], Zinc Oxide (ZnO)[8], [9], Gallium Arsenide (GaAs)[10], and Lead Zirconate Titanate (PZT)[8], [11]. Solidly mounted resonators (SMR) and thin-film bulk acoustic resonators (FBAR) have been successfully employed in Radio Frequency (RF) applications utilizing a CMOS compatible sputtering process[12]. AlN-based FBAR is famous for its high electromechanical coupling coefficient and quality factor[12]. However, it is challenging to achieve multi-frequency tunability in one chip. Thanks to its chip-scale multiple operating frequencies by lithographically defined interdigitated electrode pitches, AlN-based lamb wave resonator (LWR) have been reported as one of the most promising approaches to achieving multi-band application in 5G communication[1], [13], [14].

Recently, Aluminum Scandium Nitride (AlScN) thin film has become one of the promising methods for boosting the electromechanical coefficient of resonators[15]–[17]. In Sc-doped AlN thin film, some concentrations of aluminum atoms are replaced by scandium atoms. The volume of the scandium atom is larger than the aluminum atom, which contributes to a larger Sc-N-Al bond angle and length[18]. Such optimized lattice structure results in improving the piezoelectric coefficient, especially d_{33} and d_{31} piezoelectric coefficients. However, the deposition and etching of high concentration AlScN thin film are two challenging processes. The poor film quality and non-vertical etching profile result in limited electromechanical coefficient and quality factor of the device.

In this work, $Al_{0.78}Sc_{0.22}N$-based 1-port lamb wave resonator is demonstrated. The $Al_{0.78}Sc_{0.22}N$ thin film with a 1.8° FWHM of (0002) polarization is obtained by the magnetron sputtering process. Inductively Coupled Plasma (ICP) etching optimization process is discussed. An optimized etching recipe with a high etching rate of over 120 nm/min and a vertical etching boundary of 77° is achieved. Finally, a high-performance $Al_{0.78}Sc_{0.22}N$ lamb wave resonator with floating metal is fabricated and characterized, yielding a k_t^2 of 5.24% and Q_{loaded} of 1219.

II. Fabrication

A. $Al_{0.78}Sc_{0.22}N$ thin film co-sputtering

500 nm (0002) polar $Al_{0.78}Sc_{0.22}N$ thin film is grown on the high-resistive silicon wafer using EVATEC CLN200 co-sputtering system. Compared to the AlScN sputtering with single alloy target, co-sputtering takes advantage of tuning the power ratio of scandium and aluminum target to achieve

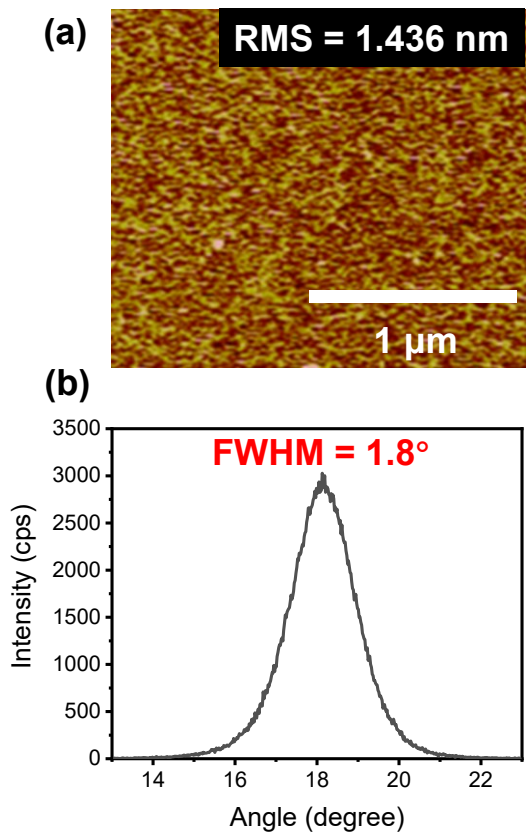

Fig. 1. (a)AFM height image of $Al_{0.78}Sc_{0.22}N$ surface. (b) rocking curve of $Al_{0.78}Sc_{0.22}N$ thin film by X-ray diffraction.

2021 IEEE International Ultrasonics Symposium (IUS) | 978-1-6654-0355-9/21/$31.00 ©2021 IEEE | DOI: 10.1109/IUS52206.2021.9593409

different concentrations in $Al_{1-x}Sc_xN$ thin film. The deposition temperature is set to 350 °C. The atomic focus microscope (AFM) height image is illustrated in Fig. 1(a). The root-mean-square (RMS) value is 1.436 nm. As shown in Fig. 1(b), the full-width-at-half-maximum (FWHM) of rocking curve is 1.8°.

B. *$Al_{0.78}Sc_{0.22}N$ thin film ICP etching*

The co-sputtered $Al_{0.78}Sc_{0.22}N$ thin film is etched by $Cl_2/BCl_3/N_2$ mixed gas[19]. Compared to the pure AlN film, the etch rate and selectivity of $Al_{0.78}Sc_{0.22}N$ film usually drop significantly using a recipe without optimization. The optimization of RF power in ICP etching is delivered in Fig. 2. RF power can control the energy plasma bombarding to the sample. During the etching process, $ScCl_3$ non-volatile byproduct will cover the etching surface, which contributes to a low etch rate. RF power is increased to both increase the possibility of Sc-N and Al-N bond-breaking by chemical reaction, and enhance the physical bombardment by increase the energy of BCl_3/N_2 then remove the $ScCl_3$ from surface. According to these two aspects, the etch rate increases. The higher RF power also results in a more vertical sidewall, due to the directionality of the etchants. When RF power is increased from 250 W to 350 W, etch rate, selectivity, and profile are developed effectively. Over 120 nm/min etch rate, 77° etch profile and nearly 1:1 selectivity are achieved utilizing optimized ICP etching recipe.

C. *$Al_{0.78}Sc_{0.22}N$ lamb wave resonators*

The lamb wave resonators are fabricated through a three-mask process on a high-resistive silicon wafer[2]. First, 10 nm Ti/ 100 nm Pt is deposited utilizing physical vapor deposition (PVD) and then patterned as bottom floating electrode via lift-off process. Then, 500 nm $Al_{0.78}Sc_{0.22}N$ thin film is deposited by a co-sputtering process. 2 µm SiO_2 is deposited by plasma enhanced chemical vapor deposition (PECVD) and patterned as a hard mask. Then, The ICP etching of $Al_{0.78}Sc_{0.22}N$ is used to define the boundary of resonators. Next, 200 nm aluminum layer is patterned as top interdigital electrodes (IDT). Finally, the $Al_{0.78}Sc_{0.22}N$ lamb wave resonators are released by XeF_2.

III. Results and Discussions

The simulated admittance response and quality factor is obtained utilizing 3D perfectly matched layer (PML) based finite element analysis (FEA) simulation in COMSOL Multiphysics®. The material constants of $Al_{0.78}Sc_{0.22}N$ used in the simulation is calculated and shown in Table I. The design of the anchor dimension is vital to the lamb wave resonator. The appropriate design can effectively reduce the anchor loss and improve the quality factor of resonators. Fig. 3 (a) shows the displacement fields of $Al_{0.78}Sc_{0.22}N$ lamb wave resonator with an anchor length of 23 µm operating at S_0 mode. According to the displacement fields, most energy is confined in the main vibration region, and a few acoustic wave is leaked into $Al_{0.78}Sc_{0.22}N$ plate through the anchor. Fig. 3 (b) illustrates the simulated admittance response and quality factor of $Al_{0.78}Sc_{0.22}N$ lamb wave resonator with three different anchor designs. The best performance is found for the anchor with a length of 23 µm, the quality factor exceeds 3496, which is 54 % higher compared to the lamb wave resonators with an anchor length equal to 28 µm. According to the abovementioned theoretical analysis, our $Al_{0.78}Sc_{0.22}N$ lamb wave resonator is designed with an anchor length equal to 23 µm.

According to the fabrication process discussed in Section II, the $Al_{0.78}Sc_{0.22}N$ lamb wave resonator with an anchor length of 23 µm is fabricated. The admittance spectra of resonator measured by Keysight® PNA-L N5234B network analyzer is shown in Fig. 4. Insert optical picture shows the device

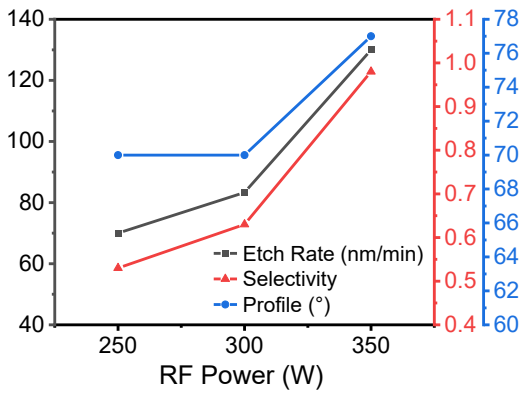

Fig. 2. ICP etch rate, selectivity and profile versus the RF power.

TABLE I. Material constants of $AL_{0.78}Sc_{0.22}N$

e_{15} (C/m^2)	-0.3104	C_{11} (GPa)	317
e_{31} (C/m^2)	-0.4992	C_{12} (GPa)	131
e_{33} (C/m^2)	1.9158	C_{13} (GPa)	115
C_{33} (GPa)	250	C_{44} (GPa)	99

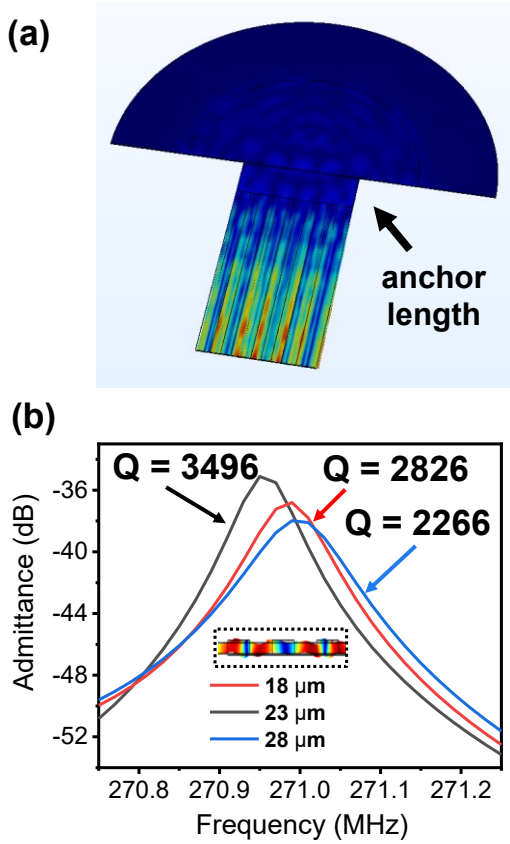

Fig. 3. (a) Simulated displacement fields of S_0 mode $Al_{0.78}Sc_{0.22}N$ lamb wave resonator with anchor length equal to 23 µm. (b) Simulated admittance response and Q value of $Al_{0.78}Sc_{0.22}N$ lamb wave resonator with different anchor designs.

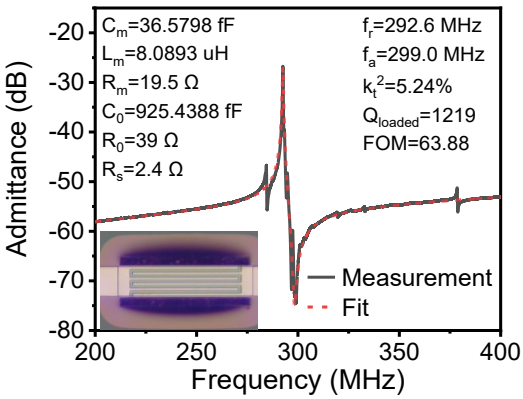

Fig. 4. Measured admittance response of $Al_{0.78}Sc_{0.22}N$ lamb wave resonator with anchor length of 23 μm.

structure with 3-pair electrodes. The $Al_{0.78}Sc_{0.22}N$ lamb wave resonator operates at around 300 MHz, yielding a k_t^2 of 5.24% and Q_{loaded} of 1219. The admittance response of resonator is fitted by the modified Butterworth-Van Dyke (mBVD) model. The extracted electric parameters are listed in Fig. 4, where C_m, L_m, R_m are the motional capacitance, inductance, and resistance of resonators, respectively, and R_s is the loaded resistance in series, C_0 and R_0 are the static capacitance and resistance of the resonator, respectively. The electro-mechanical coefficient is measured by (1), and loaded quality factor is characterized by (2).

$$k_t^2 = \frac{\pi^2}{8} \times \frac{(f_a^2 - f_r^2)}{f_r^2} \quad (1)$$

$$Q_{loaded} = \frac{f_r}{f_{3dB}} \quad (2)$$

Where f_r and f_a are the resonant and anti-resonant frequencies, respectively. f_{3dB} is the 3 dB bandwidth of resonant frequency. The resonant frequency of AlN lamb wave resonator with the same dimension of piezoelectric film and electrodes is about 380 MHz. in other words, the phase velocity of S_0 mode with the pitch of 24 μm is decreased from 9000 m/s to 8000 m/s when the piezoelectric layer changes from pure AlN to $Al_{0.78}Sc_{0.22}N$. Such reduction in phase velocity is appeared by the softening in stiffness coefficient.

IV. Conclusion

In this paper, we report a 1-port $Al_{0.78}Sc_{0.22}N$ lamb wave resonator. The high-quality $Al_{0.78}Sc_{0.22}N$ thin film is obtained utilizing magnetron co-sputtering process with FWHM of 1.8°. The characterization of ICP etching process is discussed. The etch rate of 120 nm/min and etch profile of 77° are achieved using an optimized etching recipe. This work shows a high k_t^2 of 5.24%, which is 2× higher than the lamb wave resonator with pure AlN thin film. The Q_{loaded} of 1219 is also obtained by design the dimension of the anchor to reduce energy loss.

Acknowledgment

This work was supported from the ShanghaiTech Quantum Device Lab (SQDL), and Analytical Instrumentation Center (SPSTAIC10112914) XRD Lab, School of Physical Sciences and Technology, ShanghaiTech University, Natural Science Foundation of Shanghai (19ZR1477000) and National Natural Science Foundation of China (61874073).

References

[1] T. Wu, G. Chen, C. Cassella, W. Z. Zhu, M. Assylbekova, M. Rinaldi, N. McGruer, "Design and fabrication of AlN RF MEMS switch for near-zero power RF wake-up receivers," in *2017 IEEE SENSORS*, Oct. 2017, pp. 1–3.

[2] A. Gao, K. Liu, J. Liang, T. Wu, "AlN MEMS filters with extremely high bandwidth widening capability," *Microsyst Nanoeng*, vol. 6, no. 1, p. 74, Dec. 2020.

[3] T. Yokoyama, Y. Iwazaki, Y. Onda, T. Nishihara, Y. Sasajima, M. Ueda, "Highly piezoelectric co-doped AlN thin films for wideband FBAR applications," *IEEE Transactions on Ultrasonics, Ferroelectrics, and Frequency Control*, vol. 62, no. 6, Art. no. 6, Jun. 2015.

[4] G. Piazza, P. J. Stephanou, A. P. Pisano, "Single-Chip Multiple-Frequency ALN MEMS Filters Based on Contour-Mode Piezoelectric Resonators," *J. Microelectromech. Syst.*, vol. 16, no. 2, pp. 319–328, Apr. 2007.

[5] M.-A. Dubois, P. Muralt, "Properties of aluminum nitride thin films for piezoelectric transducers and microwave filter applications," *Applied Physics Letters*, vol. 74, no. 20, Art. no. 20, 1999.

[6] L. Colombo, A. Kochhar, G. Vidal-Alvarez, G. Piazza, "X-Cut Lithium Niobate Laterally Vibrating MEMS Resonator With Figure of Merit of 1560," *J. Microelectromech. Syst.*, vol. 27, no. 4, pp. 602–604, Aug. 2018.

[7] J. D. Witmer, J. A. Valery, P. Arrangoiz-Arriola, C. J. Sarabalis, J. T. Hill, A. H. Safavi-Naeini, "High-Q photonic resonators and electro-optic coupling using silicon-on-lithium-niobate," *Sci Rep*, vol. 7, no. 1, p. 46313, May 2017.

[8] Q.-X. Su, P. Kirby, E. Komuro, M. Imura, Q. Zhang, R. Whatmore, "Thin-film bulk acoustic resonators and filters using ZnO and lead-zirconium-titanate thin films," *IEEE Trans. Microwave Theory Techn.*, vol. 49, no. 4, pp. 769–778, Apr. 2001.

[9] L. Rana, R. Gupta, M. Tomar, V. Gupta, "ZnO/ST-Quartz SAW resonator: An efficient NO2 gas sensor," *Sensors and Actuators B: Chemical*, vol. 252, pp. 840–845, Nov. 2017.

[10] H. Yamaguchi, "GaAs-based micro/nanomechanical resonators," *Semicond. Sci. Technol.*, vol. 32, no. 10, p. 103003, Sep. 2017.

[11] M.-H. Li, C.-Y. Chen, R. Lu, Y. Yang, T. Wu, S. Gong, "Power-Efficient Ovenized Lithium Niobate SH0 Resonator Arrays with Passive Temperature Compensation," in *2019 IEEE 32nd International Conference on Micro Electro Mechanical Systems (MEMS)*, Seoul, Korea (South), Jan. 2019, pp. 911–914.

[12] R. Ruby, P. Bradley, J. D. Larson, Y. Oshmyansky, "PCS 1900 MHz duplexer using thin film bulk acoustic resonators (FBARs)," *Electronics Letters*, vol. 35, no. 10, Art. no. 10, 1999.

[13] M. Rinaldi, C. Zuniga, Chengjie Zuo, G. Piazza, "Super-high-frequency two-port AlN contour-mode resonators for RF applications," *IEEE Trans. Ultrason., Ferroelect., Freq. Contr.*, vol. 57, no. 1, pp. 38–45, Jan. 2010.

[14] A. Ansari, "Single Crystalline Scandium Aluminum Nitride: An Emerging Material for 5G Acoustic Filters," in *2019 IEEE MTT-S International Wireless Symposium (IWS)*, May 2019, pp. 1–3.

[15] S. Barth, H. Bartzsch, D. Gloess, P. Frach, T. Herzog, S. Walter, H. Heuer, "Sputter deposition of stress-controlled piezoelectric AlN and AlScN films for ultrasonic and energy harvesting applications," *IEEE Transactions on Ultrasonics, Ferroelectrics, and Frequency Control*, vol. 61, no. 8, Art. no. 8, Aug. 2014.

[16] M. Akiyama, T. Kamohara, K. Kano, A. Teshigahara, Y. Takeuchi, N. Kawahara, "Enhancement of Piezoelectric Response in Scandium Aluminum Nitride Alloy Thin Films Prepared by Dual Reactive Cosputtering," *Advanced Materials*, vol. 21, no. 5, Art. no. 5, 2008.

[17] S. Shao, Z. Luo, T. Wu, "High Figure-of-Merit Lamb Wave Resonators Based on Al0. 7Sc0. 3N Thin Film," *IEEE Electron Device Letters*, vol. 42, no. 9, pp. 1378–1381, 2021.

[18] Y. Lu, M. Reusch, N. Kurz, A. Ding, T. Christoph, M. Prescher, L. Kirste, O. Ambacher, A. Žukauskaitė, "Elastic modulus and coefficient of thermal expansion of piezoelectric $Al_{1-x}Sc_xN$ (up to x = 0.41) thin films," *APL Materials*, vol. 6, no. 7, Art. no. 7, Jul. 2018.

[19] Z. Luo, S. Shao, T. Wu, "Characterization of AlN and AlScN film ICP etching for micro/nano fabrication," *Microelectronic Engineering*, p. 111530, Feb. 2021.